

Nonequilibrium inhomogeneous steady state distribution in disordered, mean-field rotator systems

Alessandro Campa¹, Shamik Gupta², and Stefano Ruffo²

¹ Complex Systems and Theoretical Physics Unit, Health and Technology Department, Istituto Superiore di Sanità, and INFN Roma1, Gruppo Collegato Sanità, Viale Regina Elena 299, 00161 Roma, Italy

² Dipartimento di Fisica e Astronomia and CSDC, Università di Firenze, INFN and CNISM, via G. Sansone, 1 50019 Sesto Fiorentino, Italy

E-mail:

`alessandro.campa@iss.infn.it, shamikg1@gmail.com, stefano.ruffo@gmail.com`

Abstract. We present a novel method to compute the phase space distribution in the nonequilibrium stationary state of a wide class of mean-field systems involving rotators subject to quenched disordered external drive and dissipation. The method involves a series expansion of the stationary distribution in inverse of the damping coefficient; the expansion coefficients satisfy recursion relations whose solution requires computing a matrix where about three quarters of the elements vanish, making numerical evaluation simple and efficient. We illustrate our method for the paradigmatic Kuramoto model of spontaneous collective synchronization and for its two mode generalization, in presence of noise and inertia, and demonstrate an excellent agreement between simulations and theory for the phase space distribution.

PACS numbers: 05.45.Xt, 05.70.Ln, 02.50.-r

Contents

1	Introduction	2
2	The class of models	4
3	The Kramers equation and its stationary solutions	6
3.1	Solution of the system of equations (30)	9
4	Illustration for a representative example: The Kuramoto interaction potential	12
5	Conclusions	15
	Acknowledgments	15
	Appendix: Convergence properties of the density expansion	16
	References	17

1. Introduction

Spontaneous collective synchronization in a large population of coupled oscillators of varying frequencies occurs in a wide variety of systems spanning length and time scales of several orders of magnitude. Examples are yeast cell suspensions [1], cardiac cells [2], fireflies [3], Josephson junctions [4], atomic recoil lasers [5], animal flocks [6], pedestrian motion on footbridges [7], audience applause in concert halls [8], and many others [9]. The paradigmatic minimal model to study synchrony and its emergence from asynchronous/incoherent phase is the celebrated Kuramoto model, involving phase-only oscillators of distributed natural frequencies coupled via a mean field [10, 11]. The model enjoys the status of one of the most studied nonlinear dynamical systems, which continues to provoke many unresolved issues [12].

In the Kuramoto model, the oscillator phases follow a first-order evolution in time. A generalized second-order stochastic dynamics, initially studied to model better synchronization among flashing fireflies, accounts for the finite moments of inertia of the oscillators (thus, the oscillators become instead the rotators), and for the stochastic fluctuations of the natural frequencies in time [13–15]. The generalized dynamics without stochasticity also arises in electrical power distribution networks [16, 17].

In a different context, one may interpret the generalized Kuramoto dynamics as that of a system of interacting particles driven by quenched disordered external torques, and evolving in presence of an external heat bath and dissipation; the Kuramoto model is

recovered as the overdamped, noiseless dynamics. This interpretation offers the very promising possibility of studying the dynamics from statistical mechanical perspectives by using tools of kinetic theory [18, 19]. The generalized model is a rich laboratory to study many-body nonequilibrium dynamics in presence of external drive and quenched disorder. The system relaxes at long times to a nonequilibrium stationary state (NESS) [18, 19]; the synchronized state (respectively, the incoherent state) corresponds to a spatially inhomogeneous (respectively, spatially homogeneous) NESS.

Unlike in equilibrium, a NESS is characterized by a violation of detailed balance, and an associated phase space distribution that cannot be expressed in the Gibbs-Boltzmann form $\sim \exp(-\beta H)$ in terms of a Hamiltonian H and an inverse temperature β . Instead, the NESS distribution has to be obtained by studying on a case-by-case basis the underlying dynamical model. This task proves daunting especially for many-body interacting systems; exact results are known only for simple models, often via *tour de force* [20], while for more complex models, simulations and approximation methods are invoked [21].

In this paper, we provide a novel method to obtain the inhomogeneous NESS single-rotator phase space distribution for the generalized Kuramoto model in the thermodynamic limit. The resulting distribution has a nontrivial form with respect to the Gibbs-Boltzmann distribution in equilibrium. Our result provides an example of a computation of a nontrivial probability distribution associated to a NESS in presence of quenched disorder. Significantly, our proposed method applies not just to the case at hand, but, in fact, to *any* periodic two-body mean-field interaction potential, thereby providing a general framework to compute NESS distribution in a wide class of systems.

Our method involves a series expansion of the stationary distribution in terms of the inverse of the damping coefficient, as opposed to an expansion in the same parameter of the Kramers operator for the time evolution of the single-rotator distribution [22]. In our method, the expansion coefficients satisfy recursion relations whose solution requires evaluation of a matrix where about three quarters of the elements vanish, making the numerical implementation very efficient computationally and also simple compared to the operator-expansion method. Also, in contrast to application of the latter method to systems in external fields [22], we develop our method for mean-field systems that require self-consistent evaluation of the mean fields. Note that the series expansion of the distribution is asymptotic in nature (just as the expansion of the Kramers operator [22]), and one can resort to the Borel summation method to sum the series properly [23]. In the context of the generalized Kuramoto dynamics, we demonstrate an excellent agreement of our theory with simulation results for the phase space distribution. The latter is characterized by a spatially non-uniform temperature profile distinctive of NESSs and absent in equilibrium.

We remark that in a recent work [18] we studied the generalized Kuramoto dynamics, with a focus on obtaining the complete phase diagram of the model for a general unimodal frequency distribution of the oscillators. Based on simulations and some analytic bounds,

we demonstrated that the model shows a nonequilibrium first-order phase transition from a synchronized phase at low values of the relevant parameters to an incoherent phase at high values. However, our analytical approach allowed to obtain only the homogeneous NESS single-rotator phase space distribution and to study its dynamical stability, while we could not compute analytically the distribution of the inhomogeneous NESS, namely, the synchronized state. In the present work we do not address the issue of phase transitions, but we focus on a method that computes the inhomogeneous NESS, not just for the Kuramoto potential, but for any other periodic mean-field interaction potential. Thus, we also fill the gap left in our previous work.

The paper is organized as follows. In the following section, we state the setting of the class of mean-field models that forms the object of our study, and write the dynamical equations in a convenient dimensionless form. In Section 3, we discuss the Kramers equation for the time evolution of the single-rotator phase space distribution, and in particular, present in detail our method to compute its stationary solution for the inhomogeneous phase. Some of the technical details are relegated to the Appendix. In Section 4, we illustrate our method by considering the representative case of the Kuramoto interaction potential, and demonstrate an excellent agreement between theory and simulations for several physically relevant observables. The paper ends with conclusions.

2. The class of models

We now turn to deriving our results, by first stating the setting of the generalized Kuramoto dynamics: We have N globally coupled rotators of same moment of inertia m , with the i th rotator, $i = 1, 2, \dots, N$, having its natural frequency ω_i a quenched random variable given by a common distribution $\mathcal{G}(\omega)$. The phases θ_i 's $\in [0, 2\pi]$ and the angular velocities v_i 's follow the equations [14, 15]

$$\frac{d\theta_i}{dt} = v_i \tag{1}$$

$$m \frac{dv_i}{dt} = -\gamma v_i + \gamma \omega_i - \frac{K}{N} \sum_{j=1}^N \frac{\partial u(\theta_j - \theta_i)}{\partial \theta_i} + \sqrt{D} \eta_i(t),$$

where γ is the damping coefficient, K is the coupling constant that is scaled down by N to have a well-defined behavior of the associated term in the thermodynamic limit $N \rightarrow \infty$, $u(\theta_i - \theta_j)$ is the two-body mean-field interaction potential [24], while η_i is a Gaussian white noise:

$$\langle \eta_i(t) \rangle = 0, \quad \langle \eta_i(t) \eta_j(t') \rangle = 2\delta_{ij} \delta(t - t'). \tag{2}$$

Here, the angular brackets denote averaging with respect to noise realizations. The constant D in Eq. (1) quantifies the strength of the noise force. Noting that $u(\theta)$ is periodic and even

in θ [25], and taking $u(0) = 0$ without loss of generality, a Fourier expansion yields

$$u(\theta) = \sum_{s=1}^{\infty} \tilde{u}_s [1 - \cos(s\theta)]. \quad (3)$$

The Kuramoto potential corresponds to the choice $\tilde{u}_1 = 1, \tilde{u}_{s>1} = 0$. The noiseless ($D = 0$), overdamped ($m/\gamma \rightarrow 0$) limit recovers the Kuramoto dynamics [10, 11]:

$$\frac{d\theta_i}{dt} = \omega_i + \frac{\tilde{K}}{N} \sum_{j=1}^N \sin(\theta_j - \theta_i), \quad (4)$$

where $\tilde{K} \equiv K/\gamma$.

Common to studies of the Kuramoto model, we consider a unimodal $\mathcal{G}(\omega)$, i.e., one which is symmetric about a single maximum (same as the average $\langle \omega \rangle$), and with width σ . The dynamics (1) is invariant under $\theta_i \rightarrow \theta_i + \langle \omega \rangle t, v_i \rightarrow v_i + \langle \omega \rangle, \omega_i \rightarrow \omega_i + \langle \omega \rangle$, and the effects of σ may be made explicit by replacing ω_i in the second equation with $\sigma \omega_i$. We consider from now on the dynamics (1) with $\omega_i \rightarrow \sigma \omega_i$, and take $\mathcal{G}(\omega)$ to have zero mean and unit width, without loss of generality.

On interpreting the model (1) as that of interacting particles, m becomes the mass, θ_i the angular coordinate for the motion along a unit circle, v_i the angular velocity, and $\gamma \omega_i$ the quenched disordered external torque [18, 19]. Introduced to mimic fluctuations of the natural frequencies [26], the Gaussian noise can also be interpreted as fluctuations due to coupling to a heat bath at temperature T , and one may invoke the fluctuation-dissipation relation to relate the strength of the noise to the temperature T , as $D = \gamma k_B T$ [27]. In this case, Eq. (1) in the absence of the ω_i 's describes the dynamics of a Hamiltonian system in contact with a heat bath, and the stationary state is in equilibrium, with probability of configurations $\sim \exp(-H/T)$, where H is the Hamiltonian

$$H = \sum_{i=1}^N \frac{p_i^2}{2m} + \frac{K}{2N} \sum_{i,j=1}^N u(\theta_i - \theta_j), \quad (5)$$

with $p_i \equiv m v_i$ the angular momentum of the i -th particle. In presence of ω_i 's, the dynamics relaxes to a NESS [18, 19].

It is convenient for further analysis to write Eq. (1) in a dimensionless form. Introducing dimensionless variables

$$\bar{t} \equiv t \sqrt{K/m}, \quad (6)$$

$$\bar{v}_i \equiv v_i \sqrt{m/K}, \quad (7)$$

$$1/\sqrt{\bar{m}} \equiv \gamma/\sqrt{Km}, \quad (8)$$

$$\bar{\sigma} \equiv \gamma\sigma/K, \quad (9)$$

$$\bar{T} \equiv T/K, \quad (10)$$

$$\bar{\eta}_i(\bar{t}) \equiv \eta_i(t) \sqrt{\gamma T/K}, \quad (11)$$

Eq. (1) becomes

$$\frac{d\theta_i}{d\bar{t}} = \bar{v}_i, \quad (12)$$

$$\frac{d\bar{v}_i}{d\bar{t}} = \frac{-\bar{v}_i}{\sqrt{\bar{m}}} + \sum_{s=1}^{\infty} s\tilde{u}_s R_s \sin(s\psi - s\theta_i) + \bar{\sigma}\omega_i + \left(\frac{\bar{T}}{\sqrt{\bar{m}}}\right)^{1/2} \bar{\eta}_i(\bar{t}),$$

where

$$R_s(t)e^{is\psi(t)} \equiv \frac{1}{N} \sum_{j=1}^N e^{is\theta_j(t)}, \quad (13)$$

and the noise satisfies

$$\langle \bar{\eta}_i(\bar{t}) \bar{\eta}_j(\bar{t}') \rangle = 2\delta_{ij} \delta(\bar{t} - \bar{t}'). \quad (14)$$

For $m = 0$, using dimensionless time

$$\bar{t} \equiv t(K/\gamma), \quad (15)$$

the dynamics (1) becomes the overdamped motion

$$\frac{d\theta_i}{d\bar{t}} = \sum_{s=1}^{\infty} s\tilde{u}_s R_s \sin(s\psi - s\theta_i) + \bar{\sigma}\omega_i + \sqrt{\bar{T}} \bar{\eta}_i(\bar{t}), \quad (16)$$

which in the case $\tilde{u}_1 = 1, \tilde{u}_{s>1} = 0$ and at $\bar{T} = 0$ becomes the Kuramoto dynamics. Associated with the s th Fourier mode of the interaction potential is the magnitude of the mean field R_s acting on one rotator due to its interaction with all the others, while $s\psi$ is the corresponding phase. In particular, R_1 measures complete phase coherence among all the rotators, and its stationary value $R_1^{\text{st}} \equiv R_1(t \rightarrow \infty)$ serves as the synchronization order parameter. From now on, we consider the dynamics (12) that, besides N , depends on the parameters \bar{m} , \bar{T} , and $\bar{\sigma}$; we will drop the overbars for notational simplicity. Note that dynamics (12) reduces to dynamics (16) in the overdamped limit.

In the next section, we discuss the Kramers equation for the time evolution of the single-rotator phase space distribution, and in particular, our method to compute its stationary solutions.

3. The Kramers equation and its stationary solutions

In the thermodynamic limit, the dynamics (12) is described by the single-rotator phase space distribution $f(\theta, v, \omega, t)$, giving at time t for each ω the distribution probability of rotators with phase θ and angular velocity v . We have

$$f(\theta, v, \omega, t) = f(\theta + 2\pi, v, \omega, t), \quad (17)$$

and the normalization

$$\int d\theta dv f(\theta, v, \omega, t) = 1 \quad \forall \omega. \quad (18)$$

The time evolution of f , obtained by truncating to lowest order in $1/N$ the Bogoliubov-Born-Green-Kirkwood-Yvon (BBGKY) hierarchy equations, follows the Kramers equation [18]

$$\frac{\partial f}{\partial t} = -v \frac{\partial f}{\partial \theta} + \frac{T}{\sqrt{m}} \frac{\partial^2 f}{\partial v^2} + \frac{\partial}{\partial v} \left[\left(\frac{v}{\sqrt{m}} - \sum_{s=1}^{\infty} s \tilde{u}_s R_s \sin(s\psi - s\theta) - \sigma\omega \right) f \right], \quad (19)$$

where

$$R_s(t) e^{is\psi(t)} = \int d\theta dv d\omega \mathcal{G}(\omega) e^{is\theta} f(\theta, v, \omega, t). \quad (20)$$

We are interested in the stationary state solutions of the Kramers equation, obtained by setting the left hand side of Eq. (19) to 0. As already mentioned, the stationary state is a NESS, unless $\sigma = 0$. In the stationary state R_s and ψ are time independent; ψ can be set equal to 0 by redefining the origin of the θ_i 's, while with R_s^{st} we will denote the stationary value of R_s . We will also use the definition

$$G(\theta) \equiv \sum_{s=1}^{\infty} s \tilde{u}_s R_s^{\text{st}} \sin(s\theta). \quad (21)$$

The θ -independent solution characterizing the incoherent phase, for which $R_s^{\text{st}} = 0 \quad \forall s$ and thus $G(\theta) = 0$, is given by [14]:

$$f^{\text{inc}}(\theta, v, \omega) = \frac{1}{2\pi} \sqrt{\frac{1}{2\pi T}} \exp \left[-\frac{(v - \sigma\omega\sqrt{m})^2}{2T} \right]. \quad (22)$$

The synchronized phase distribution for $\sigma = 0$ is given by the Gibbs-Boltzmann measure $\sim \exp[-v^2/(2T) - \int d\theta G(\theta)]$; for general σ , we expand it as

$$f^{\text{syn}}(\theta, v, \omega) = \Phi_0 \left(\frac{v}{\sqrt{2T}} \right) \sum_{n=0}^{\infty} b_n(\theta, \omega) \Phi_n \left(\frac{v}{\sqrt{2T}} \right), \quad (23)$$

where the functions b_n 's satisfy $b_n(\theta, \omega) = b_n(\theta + 2\pi, \omega)$, while $\Phi_n(ax)$ is the Hermite function:

$$\Phi_n(ax) = \sqrt{\frac{a}{2^n n! \sqrt{\pi}}} \exp \left[-\frac{a^2 x^2}{2} \right] H_n(ax), \quad (24)$$

with $H_n(x)$'s being the n -th degree Hermite polynomial. The functions Φ_n 's are orthonormal: $\int dx \Phi_m(ax) \Phi_n(ax) = \delta_{mn}$. Normalization of $f^{\text{syn}}(\theta, v, \omega)$ implies that $\int_0^{2\pi} d\theta b_0(\theta, \omega) = 1$, while the self-consistent values of the parameters R_s^{st} are given by

$$R_s^{\text{st}} = \int d\omega \mathcal{G}(\omega) \int_0^{2\pi} d\theta b_0(\theta, \omega) e^{is\theta}. \quad (25)$$

Furthermore, using $\int dx x\Phi_0(ax)\Phi_n(ax) = 1/(\sqrt{2}a)\delta_{n,1}$, we obtain that

$$\int dv v f^{\text{syn}}(\theta, v, \omega) = \sqrt{T}b_1(\theta, \omega). \quad (26)$$

On the other hand, integrating over v the stationary state Kramers equation, we obtain that $\int dv v f^{\text{syn}}(\theta, v, \omega)$ and, hence, $b_1(\theta, \omega)$, does not depend on θ .

The choice of the Hermite functions in the expansion (23) is motivated by the fact for $\sigma = 0$, the distribution $f_{\text{syn}}(\theta, v, \omega)$ should have the Gibbs-Boltzmann form, $f_{\text{syn}}(\theta, v, \omega) \sim \exp[-v^2/(2T) - \int d\theta G(\theta)]$. As will be shown later, the expansion coefficients b_n for this case satisfy $b_0(\theta, 0) \sim \exp[-\int d\theta G(\theta)]$, $b_n(\theta, 0) = 0$ for $n > 0$, so that only the $n = 0$ term in the expansion (23) needs to be taken into account; then, with $\Phi_0(x) \sim \exp(-x^2/2)$, the product $\Phi_0\left(\frac{v}{\sqrt{2T}}\right)\Phi_0\left(\frac{v}{\sqrt{2T}}\right)$ appearing in the expansion correctly reproduces the velocity-part of the distribution $\sim \exp[-v^2/(2T)]$.

Plugging the expansion (23) into the stationary state Kramers equation, using the known recursion relations for the Hermite polynomials, and equating to zero the coefficient of each Φ_n , we get

$$\sqrt{nT}\frac{\partial b_{n-1}(\theta, \omega)}{\partial \theta} + \sqrt{(n+1)T}\frac{\partial b_{n+1}(\theta, \omega)}{\partial \theta} + \frac{n}{\sqrt{m}}b_n(\theta, \omega) + \sqrt{\frac{n}{T}}b_{n-1}(\theta, \omega)[G(\theta) - \sigma\omega] = 0 \quad (27)$$

for $n = 0, 1, 2, \dots$ (with the understanding that $b_{-1}(\theta, \omega) \equiv 0$). Equation (27) is a time-independent generalized version of the Brinkman's hierarchy [22, 28, 29]. The hierarchy was introduced to study the approach to a stationary state of a system of noninteracting particles subjected to external forces and noise. We remark that in our case we have a system of interacting particles, so that the forces are both external (the driving torques) and due to an interaction potential. The equation for $n = 0$ recovers the result that $b_1(\theta, \omega)$ is independent of θ . Noting the scaling of the various terms in Eq. (27) with m , we expand $b_n(\theta, \omega)$ as

$$b_n(\theta, \omega) = \sum_{k=0}^{\infty} (\sqrt{m})^k c_{n,k}(\theta, \omega), \quad (28)$$

with $b_1(\theta, \omega)$ independent of θ implying that so is $c_{1,k}(\theta, \omega) \forall k$. The only constraint on $b_0(\theta, \omega)$ being $\int_0^{2\pi} d\theta b_0(\theta, \omega) = 1$, we may without loss of generality choose $c_{0,k \geq 1}(0, \omega) = 0$. This will prove very useful for further analysis, as will be shown below. We now use Eq. (28) in Eq. (27) and equate to zero the coefficient of each power of \sqrt{m} . The term proportional to $(\sqrt{m})^{-1}$ gives simply

$$nc_{n,0}(\theta, \omega) = 0, \quad (29)$$

which implies that $c_{n,0}(\theta, \omega) = 0$ for $n > 0$. The coefficient of the term proportional to $(\sqrt{m})^k$ leads to

$$\sqrt{nT}\frac{\partial c_{n-1,k}(\theta, \omega)}{\partial \theta} + \sqrt{(n+1)T}\frac{\partial c_{n+1,k}(\theta, \omega)}{\partial \theta} + \sqrt{nT}a(\theta, \omega)c_{n-1,k}(\theta, \omega) + nc_{n,k+1}(\theta, \omega) = 0 \quad (30)$$

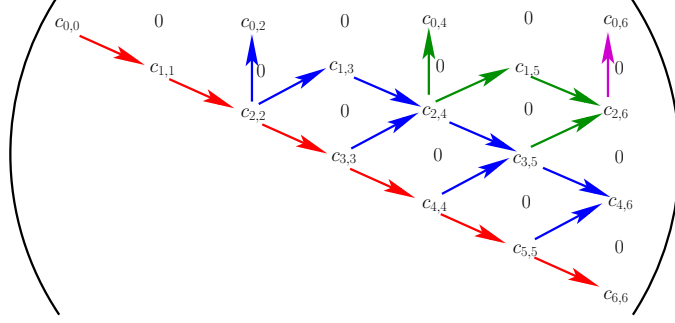


Figure 1. Flow diagram for the evaluation of the expansion coefficients $c_{n,k}(\theta, \omega)$; $n, k = 0, 1, 2, \dots, 6$. Starting from the main diagonal, arrows and different colors denote subsequent flows (see text). The elements below the main diagonal are all zero.

for $n, k = 0, 1, 2, \dots$ (with $c_{-1,k}(\theta, \omega) \equiv 0$), where $a(\theta, \omega) \equiv [G(\theta) - \sigma\omega]/T$. The system of equations (30) can be solved recursively, as we detail now.

3.1. Solution of the system of equations (30)

Let us first consider Eq. (30) for $n = 0$; we immediately obtain that $c_{1,k}(\theta, \omega)$ is independent of θ for each k , as we had already inferred above. To proceed, we consider Eq. (30) for $k = 0$ and $n = 2, 3, \dots$; since $c_{n,0}(\theta, \omega) = 0$ for $n > 0$, we get that $c_{n,1}(\theta, \omega) = 0$ for $n > 1$. Considering next the equation for $k = 1$ and $n = 3, 4, \dots$, we get $c_{n,2}(\theta, \omega) = 0$ for $n > 2$; for $k = 2$ and $n = 4, 5, \dots$ we get $c_{n,3}(\theta, \omega) = 0$ for $n > 3$, and so on. We thus arrive at the general result that $c_{n,k}(\theta, \omega) = 0 \forall k < n$. In Fig. 1, we display the coefficients $c_{n,k}$ in a matrix. The result just obtained shows that the matrix is upper triangular. We are thus left to consider Eq. (30) for $n = 1, 2, \dots$ and $k \geq n - 1$, or, equivalently, for $k = 0, 1, 2, \dots$ and $n = 1, 2, \dots, k + 1$. In what follows, we will obtain the elements of the main diagonal, $c_{n,n}(\theta, \omega)$, then the elements of the first upper diagonal, $c_{n,n+1}(\theta, \omega)$, the elements of the second upper diagonal, $c_{n,n+2}(\theta, \omega)$, and so on. Thus, let us begin by studying the case $n = 1$ and $k = 0$. We have

$$\sqrt{T} \frac{\partial c_{0,0}(\theta, \omega)}{\partial \theta} + \sqrt{2T} \frac{\partial c_{2,0}(\theta, \omega)}{\partial \theta} + \sqrt{T} a(\theta, \omega) c_{0,0}(\theta, \omega) + c_{1,1}(\omega) = 0. \quad (31)$$

In this equation, $c_{2,0}(\theta, \omega) = 0$, while $c_{1,1}(\omega)$ is independent of θ . We thus have a first-order differential equation for $c_{0,0}(\theta, \omega)$, with an unknown constant. The requirement of periodicity, i.e., $c_{0,0}(\theta, \omega) = c_{0,0}(\theta + 2\pi, \omega)$, fixes the value of this constant, and we obtain

$$c_{0,0}(\theta, \omega) = c_{0,0}(0, \omega) e^{-g(\theta, \omega)} \left[1 + (e^{g(2\pi, \omega)} - 1) \frac{\int_0^\theta d\theta' e^{g(\theta', \omega)}}{\int_0^{2\pi} d\theta' e^{g(\theta', \omega)}} \right], \quad (32)$$

$$c_{1,1}(\omega) = \sqrt{T} \frac{c_{0,0}(0, \omega) (1 - e^{g(2\pi, \omega)})}{\int_0^{2\pi} d\theta' e^{g(\theta', \omega)}}, \quad (33)$$

where $g(\theta, \omega) = \int_0^\theta d\theta' a(\theta', \omega)$, and $c_{0,0}(0, \omega)$ is to be fixed at the end by the normalization of $b_0(\theta, \omega)$. Having determined $c_{0,0}(\theta, \omega)$ and $c_{1,1}(\omega)$, we then obtain recursively the main diagonal elements, by considering Eq. (30) for $n = 2, 3, \dots$ and $k = n - 1$; this gives

$$\begin{aligned} & \sqrt{nT} \frac{\partial c_{n-1, n-1}(\theta, \omega)}{\partial \theta} + \sqrt{(n+1)T} \frac{\partial c_{n+1, n-1}(\theta, \omega)}{\partial \theta} \\ & + \sqrt{nT} a(\theta, \omega) c_{n-1, n-1}(\theta, \omega) + n c_{n, n}(\theta, \omega) = 0. \end{aligned} \quad (34)$$

Since $c_{n+1, n-1}(\theta, \omega) = 0$, we have

$$c_{n, n}(\theta, \omega) = -\sqrt{\frac{T}{n}} \left[\frac{\partial c_{n-1, n-1}(\theta, \omega)}{\partial \theta} + a(\theta, \omega) c_{n-1, n-1}(\theta, \omega) \right] \quad (35)$$

for $n = 2, 3, \dots$. In particular, for $n = 2$ the first term within the square brackets is absent, since $c_{1,1}(\omega)$ is independent of θ . We note that all the functions $c_{n,n}(\theta, \omega)$ are proportional to $c_{0,0}(0, \omega)$.

We now determine the elements of the first upper diagonal. We consider Eq. (30) for $n = 1$ and $k = 1$:

$$\sqrt{T} \frac{\partial c_{0,1}(\theta, \omega)}{\partial \theta} + \sqrt{2T} \frac{\partial c_{2,1}(\theta, \omega)}{\partial \theta} + \sqrt{T} a(\theta, \omega) c_{0,1}(\theta, \omega) + c_{1,2}(\omega) = 0. \quad (36)$$

This equation has exactly the same structure as Eq. (31), since $c_{2,1}(\theta, \omega) = 0$, and $c_{1,2}(\omega)$ is a constant independent of θ . At this point, we use the fact that $c_{0,k}(0, \omega) = 0$ for $k \geq 1$. Then, the solution of Eq. (36) is simply $c_{0,1}(\theta, \omega) = c_{1,2}(\omega) \equiv 0$. Next, by considering Eq. (30) for $n = 2, 3, \dots$ and $k = n$, and proceeding similarly, we obtain that all the functions $c_{n, n+1}(\theta, \omega)$, i.e., the elements of the first upper diagonal of Fig. 1, vanish.

Next, we determine the elements of the second upper diagonal, beginning by considering Eq. (30) for $n = 1$ and $k = 2$:

$$\sqrt{T} \frac{\partial c_{0,2}(\theta, \omega)}{\partial \theta} + \sqrt{2T} \frac{\partial c_{2,2}(\theta, \omega)}{\partial \theta} + \sqrt{T} a(\theta, \omega) c_{0,2}(\theta, \omega) + c_{1,3}(\omega) = 0. \quad (37)$$

In this equation, $c_{2,2}(\theta, \omega)$ is known from Eq. (35). Then, from the requirement of periodicity of $c_{0,2}(\theta, \omega)$, and using $c_{0,2}(0, \omega) = 0$, we obtain the solutions

$$\begin{aligned} c_{0,2}(\theta, \omega) &= \sqrt{2} \frac{\int_0^{2\pi} d\theta' \frac{\partial c_{2,2}(\theta', \omega)}{\partial \theta'} e^{g(\theta', \omega)}}{\int_0^{2\pi} d\theta' e^{g(\theta', \omega)}} e^{-g(\theta, \omega)} \int_0^\theta d\theta' e^{g(\theta', \omega)} \\ &\quad - \sqrt{2} e^{-g(\theta, \omega)} \int_0^\theta d\theta' \frac{\partial c_{2,2}(\theta', \omega)}{\partial \theta'} e^{g(\theta', \omega)}, \end{aligned} \quad (38)$$

$$c_{1,3}(\omega) = -\sqrt{2T} \frac{\int_0^{2\pi} d\theta' \frac{\partial c_{2,2}(\theta', \omega)}{\partial \theta'} e^{g(\theta', \omega)}}{\int_0^{2\pi} d\theta' e^{g(\theta', \omega)}}. \quad (39)$$

Again, these functions are proportional to $c_{0,0}(0, \omega)$. Having determined $c_{0,2}$ and $c_{1,3}$, we obtain recursively the elements of the second upper diagonal, i.e., the functions $c_{n, n+2}$, from

Eq. (30) by considering $n = 2, 3, \dots$ and $k = n + 1$:

$$\begin{aligned} & \sqrt{nT} \frac{\partial c_{n-1, n+1}(\theta, \omega)}{\partial \theta} + \sqrt{(n+1)T} \frac{\partial c_{n+1, n+1}(\theta, \omega)}{\partial \theta} \\ & + \sqrt{nT} a(\theta, \omega) c_{n-1, n+1}(\theta, \omega) + n c_{n, n+2}(\theta, \omega) = 0. \end{aligned} \quad (40)$$

With the main diagonal elements already determined, this gives

$$\begin{aligned} c_{n, n+2}(\theta, \omega) = & - \sqrt{\frac{T}{n}} \left[\frac{\partial c_{n-1, n+1}(\theta, \omega)}{\partial \theta} + a(\theta, \omega) c_{n-1, n+1}(\theta, \omega) \right] \\ & - \frac{\sqrt{(n+1)T}}{n} \frac{\partial c_{n+1, n+1}(\theta, \omega)}{\partial \theta}, \end{aligned} \quad (41)$$

for $n = 2, 3, \dots$. In particular, for $n = 2$, the first term within the square brackets is absent as $c_{1,3}(\omega)$ is independent of θ . Also these functions are proportional to $c_{0,0}(0, \omega)$.

Next, we show that the elements of the third upper diagonal vanish. Considering now Eq. (30) for $n = 1$ and $k = 3$, we have

$$\sqrt{T} \frac{\partial c_{0,3}(\theta, \omega)}{\partial \theta} + \sqrt{2T} \frac{\partial c_{2,3}(\theta, \omega)}{\partial \theta} + \sqrt{T} a(\theta, \omega) c_{0,3}(\theta, \omega) + c_{1,4}(\omega) = 0. \quad (42)$$

In this equation, $c_{2,3}$ has been previously determined to be vanishing identically, so that the solution of the last equation is simply $c_{0,3}(\theta, \omega) = c_{1,4}(\omega) \equiv 0$. Then, considering Eq. (30) for $n = 2, 3, \dots$ and $k = n + 2$, we find that all the elements of the third upper diagonal, $c_{n, n+3}$, vanish.

At this point, the procedure of determining the coefficients $c_{n,k}$'s should be clear. All the elements of the upper diagonals of odd order vanish, this being equivalent to the fact that in the portion of each row above the main diagonal, one element every two vanishes, i.e., $c_{n, n+1+2k} \equiv 0$ for $n, k = 0, 1, 2, \dots$. All the nonvanishing elements are proportional to $c_{0,0}(0, \omega)$. The expressions for the main diagonal elements have already been given in Eqs. (32), (33) and (35). On the basis of the analysis above, we can write down the general expressions for the nonvanishing non-diagonal elements as

$$\begin{aligned} c_{0,2k}(\theta, \omega) = & \sqrt{2} \frac{\int_0^{2\pi} d\theta' \frac{\partial c_{2,2k}(\theta', \omega)}{\partial \theta'} e^{g(\theta', \omega)}}{\int_0^{2\pi} d\theta' e^{g(\theta', \omega)}} e^{-g(\theta, \omega)} \int_0^\theta d\theta' e^{g(\theta', \omega)} \\ & - \sqrt{2} e^{-g(\theta, \omega)} \int_0^\theta d\theta' \frac{\partial c_{2,2k}(\theta', \omega)}{\partial \theta'} e^{g(\theta', \omega)}, \end{aligned} \quad (43)$$

$$c_{1,1+2k}(\omega) = - \sqrt{2T} \frac{\int_0^{2\pi} d\theta' \frac{\partial c_{2,2k}(\theta', \omega)}{\partial \theta'} e^{g(\theta', \omega)}}{\int_0^{2\pi} d\theta' e^{g(\theta', \omega)}}, \quad (44)$$

$$c_{2,2+2k}(\theta, \omega) = - \sqrt{\frac{T}{2}} a(\theta, \omega) c_{1,1+2k}(\omega) - \frac{\sqrt{3T}}{2} \frac{\partial c_{3,1+2k}(\theta, \omega)}{\partial \theta}, \quad (45)$$

$$\begin{aligned} c_{n, n+2k}(\theta, \omega) = & - \sqrt{\frac{T}{n}} \left[\frac{\partial c_{n-1, n-1+2k}(\theta)}{\partial \theta} + a(\theta, \omega) c_{n-1, n-1+2k}(\theta, \omega) \right] \\ & - \frac{\sqrt{(n+1)T}}{n} \frac{\partial c_{n+1, n-1+2k}(\theta, \omega)}{\partial \theta} \quad n \geq 3, \end{aligned} \quad (46)$$

with $k = 1, 2, \dots$

We show schematically in Fig. 1 the flow of the solution up to $n = k = 6$, while that for higher values proceeds analogously. As shown, the system (30) computes progressively each element of the main diagonal, and then the elements of the second upper diagonal, each one determined by the knowledge of two previously determined elements, and so on. Each element of the matrix is proportional to $c_{0,0}(0, \omega)$, which is fixed by the normalization of f^{syn} : $\sum_{k=0}^{\infty} \int_0^{2\pi} d\theta (\sqrt{m})^{2k} c_{0,2k}(\theta, \omega) = 1$. The values of R_s^{st} have to be determined self-consistently.

We end the section by pointing out that for $\sigma = 0$, or equivalently for $\omega = 0$, the equilibrium Gibbs-Boltzmann distribution is simply recovered in our procedure. In fact, it is immediate to see that for $\omega = 0$ the solution of (27) is $b_0(\theta, 0) \sim \exp[-\int d\theta G(\theta)]$ and $b_n(\theta, 0) = 0$ for $n > 0$. Coherently with this, the solution of (30) for $\omega = 0$ is $c_{0,0}(\theta, 0) \sim \exp[-\int d\theta G(\theta)]$, with all the other $c_{n,k}(\theta, 0) = 0$ vanishing. This can be readily obtained from Eqs. (32)-(46) by the fact that $g(2\pi, 0) = 0$.

4. Illustration for a representative example: The Kuramoto interaction potential

In order to illustrate an implementation of our method, we now apply it to the Kuramoto potential. In this case, as noted above, only the first Fourier term with $s = 1$ needs to be taken into account in the interaction potential. For illustrative purpose, let us choose a representative $\mathcal{G}(\omega)$, namely, a Gaussian: $\mathcal{G}(\omega) = 1/(\sqrt{2\pi}) \exp(-\omega^2/2)$, and study two physically relevant quantities in the synchronized phase. One is the marginal θ -distribution, $n(\theta) \equiv \int_{-\infty}^{\infty} d\omega \mathcal{G}(\omega) \int_{-\infty}^{\infty} dv f^{\text{syn}}(\theta, v, \omega)$, i.e., the density profile; using the orthonormality of the Hermite functions, one gets

$$n(\theta) = \int_{-\infty}^{\infty} d\omega \mathcal{G}(\omega) b_0(\theta, \omega). \quad (47)$$

The other is the quantity $p(\theta) \equiv \int_{-\infty}^{\infty} d\omega \mathcal{G}(\omega) \int_{-\infty}^{\infty} dv v^2 f^{\text{syn}}(\theta, v, \omega)$, which is proportional to the local pressure [30]. Using again the orthonormality of the Hermite functions, one has

$$p(\theta) = T \int_{-\infty}^{\infty} d\omega \mathcal{G}(\omega) \left(\sqrt{2} b_2(\theta, \omega) + b_0(\theta, \omega) \right). \quad (48)$$

We thus need the coefficients $b_0(\theta, \omega)$ and $b_2(\theta, \omega)$, whose evaluation requires truncating the expansion (28) at suitable values k_{trunc} of k . From Fig. 1, we see that knowing $c_{2,2k}$ allows to compute $c_{0,2k}$, so it is natural to choose the same k_{trunc} for both $b_0(\theta, \omega)$ and $b_2(\theta, \omega)$.

In Fig. 2, we demonstrate an excellent agreement between theory and simulations for the density $n(\theta)$, for given values of (m, T, σ) . The simulations are performed through integration of the $2N$ equations of motion (12) by using the algorithm of Ref. [18] and timestep $\delta t = 0.01$. From the plots of the figure, it is evident that our analytical approach works very well for both small and large values of m . The agreement is confirmed also in the plot of the quantity $p(\theta)$, proportional to the local pressure, as shown in the left panel of

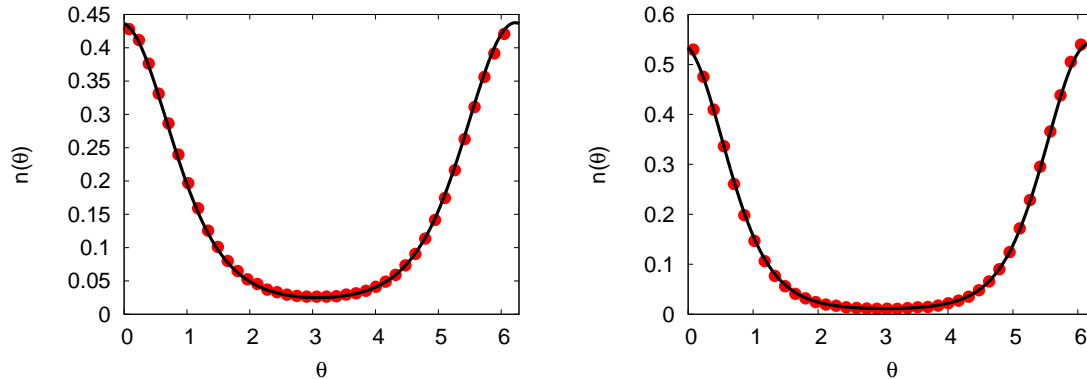


Figure 2. Density $n(\theta)$ in the dynamics (12) with $\tilde{u}_1 = 1$, $\tilde{u}_{s>1} = 0$, a Gaussian $\mathcal{G}(\omega)$, for $m = 0.25$, $T = 0.25$, $\sigma = 0.295$, $k_{\text{trunc}} = 12$ (left panel), and for $m = 5.0$, $T = 0.25$, $\sigma = 0.2$, $k_{\text{trunc}} = 2$ (right panel). Simulations (points) are for $N = 10^6$; the theoretical predictions are denoted by lines.

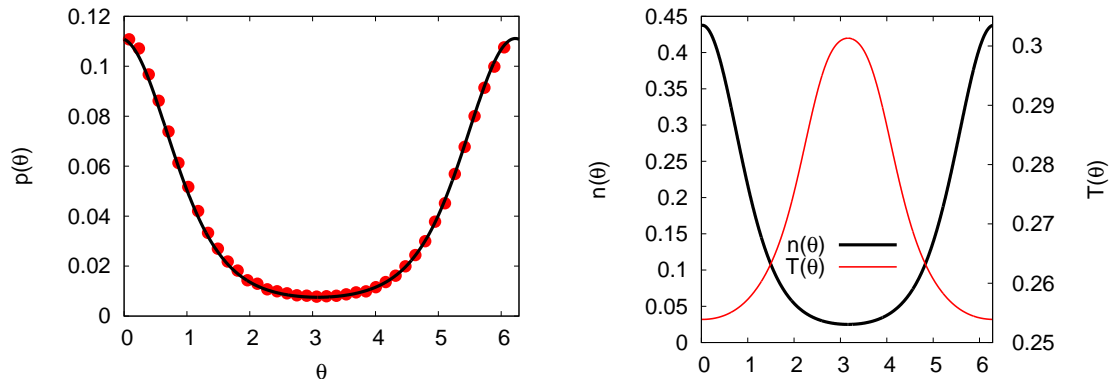


Figure 3. The left panel shows the pressure $p(\theta)$ for the same parameters as in the left panel of Fig. 2. Simulations (points) are for $N = 10^6$; the theoretical predictions are denoted by lines. The right panel shows the local temperature $T(\theta) = p(\theta)/n(\theta)$ and its anticorrelation with the density $n(\theta)$.

σ	0.0	0.05	0.1	0.15	0.2	0.25
R_1^{st} (Theory)	0.829	0.825	0.813	0.789	0.75	0.686
R_1^{st} (Simulations)	0.829	0.825	0.812	0.787	0.747	0.680

Table 1. R_1^{st} vs. σ obtained in theory and simulations in the dynamics (12), with $\tilde{u}_1 = 1$, $\tilde{u}_{s>1} = 0$, a Gaussian $\mathcal{G}(\omega)$, for several values of σ at $m = 0.25$, $T = 0.25$, $k_{\text{trunc}} = 12$.

Fig. 3, where the parameters are the same of those in the left panel of Fig. 2. As a further demonstration of the validity of our method, we list in Table 1 the value of R_1^{st} obtained in theory and simulations ($N = 10^6$) for several σ 's and $m = 0.25$, $T = 0.25$; again, we observe a very good agreement, within numerical accuracies.

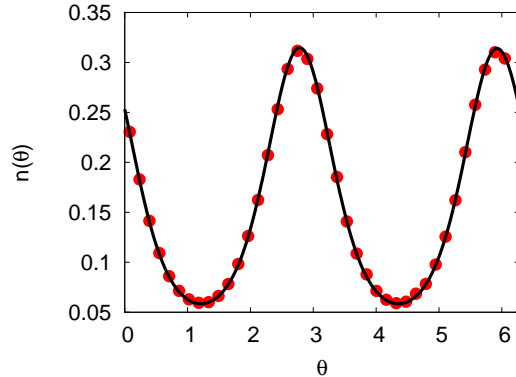


Figure 4. Density $n(\theta)$ in the dynamics (12) with $\tilde{u}_1 = 0.3$, $\tilde{u}_2 = 0.7$, $\tilde{u}_{s>2} = 0$, a Gaussian $\mathcal{G}(\omega)$, $m = 0.25$, $T = 0.25$, $\sigma = 0.295$, $k_{\text{trunc}} = 4$. Simulations (points) are for $N = 10^6$; the theoretical predictions are denoted by lines.

The ratio $p(\theta)/n(\theta)$ gives the temperature $T(\theta)$. In equilibrium, one has a spatially uniform temperature profile, i.e., $T(\theta)$ equals the temperature T of the heat bath, independent of θ . Then, the spatially non-uniform temperature profile in the right panel of Fig. 3 (where we show the theoretical computation), is a further demonstration that the synchronized state is a NESS. The panel also depicts a density-temperature anticorrelation, i.e., the temperature peaks at a θ at which the density is minimum, and vice versa. This phenomenon of temperature inversion occurs in inhomogeneous plasmas (e.g., the Solar corona [31], interstellar molecular clouds [32]), and is argued mainly by simulations to be a generic feature of long-range interacting systems in NESSs [33, 34]; here, we provide an analytic demonstration of the phenomenon.

To illustrate the generality of our method, we show in Fig. 4 the results of adding a $\cos 2\theta$ interaction to the Kuramoto potential ($\tilde{u}_1 = 0.3$, $\tilde{u}_2 = 0.7$, $\tilde{u}_{s>2} = 0$). Also in this case we see a perfect agreement of the theory with simulations.

We now discuss the behavior of the truncation order k_{trunc} in computing the density $n(\theta)$ as a function of m at a given representative (σ, T) ; in particular, we point out that Eq. (28) is an asymptotic expansion in the inverse damping coefficient \sqrt{m} . Let us consider, e.g., parameter values used in this work, i.e., $\sigma = 0.295$, $T = 0.25$ and $m = 0.25$. For these values $k_{\text{trunc}} = 18$ gives a perfect match with simulation results, as in the left panels of Fig. 2 and Fig. 3. The match is no more perfect and gets worse and worse on successively including more higher order terms in the expansion; in this case, using the Borel method [23] of summing a divergent series circumvents the problem, allowing to correctly compute $n(\theta)$ for a truncation order that in principle could be arbitrarily large. This is expected of an asymptotic expansion, and makes us conclude that Eq. (28) is an asymptotic expansion in \sqrt{m} . In the Appendix, we give some details on the Borel summation method.

5. Conclusions

We have proposed a novel method to compute the inhomogeneous NESS distribution of a wide class of mean-field systems of rotators subject to quenched disordered external drive and dissipation. We have demonstrated an excellent agreement between simulations and theory for the noisy inertial Kuramoto model of spontaneous collective synchronization, and for its two mode generalization.

Our method is based on a series expansion of the stationary distribution function $f^{\text{syn}}(\theta, v, \omega)$. First, the velocity dependence of the distribution is separated from the (θ, ω) dependence by an expansion in Hermite functions of the velocity, with coefficients functions of θ and ω (Eq. (23)); in turn, the latter functions are expanded in powers of the inverse friction constant \sqrt{m} (Eq. (28)). The second expansion is asymptotic, but we have shown that, as is generally the case with asymptotic series, we get the “right” sum by truncating at an appropriate order. Furthermore, as mentioned above and as detailed in the Appendix, one can apply the Borel summation method to sum the expansion, a method that often sums correctly an asymptotic series. We stress that the appropriate order of truncation may be found even without resorting to a comparison with simulation data, since computation with a larger order of truncation leads to numerical instabilities in the form of oscillations in the distribution, as shown in the Appendix.

We note that our method does not determine if the computed inhomogeneous stationary solution is stable for given values of the parameters. For this, it would be necessary to perform a stability analysis, which for inhomogeneous solutions is much more complicated than that for homogeneous solutions. However, by finding the inhomogeneous solutions, one can theoretically determine the hysteresis loops associated with the presence of non-equilibrium first-order phase transitions in the class of models we considered. In fact, the knowledge of the stability of the incoherent θ -independent solution (22) as a function of the parameters [19], and the determination of the synchronized coherent solution, together allow to localize the hysteresis loops in the parameter space.

To sign off, we want to stress that the method can be applied also to classes of models that generalize the one considered in this work [35, 36].

Acknowledgments

We thank M. Komarov and A. Pikovsky for discussions, and the Galileo Galilei Institute for Theoretical Physics, Florence, Italy for the hospitality and the INFN for partial support during the completion of this work.

Appendix: Convergence properties of the density expansion

Consider an asymptotic power series in the real variable x ,

$$A(x) = \sum_{k=0}^{\infty} a_k x^k, \quad (\text{A.1})$$

and define the partial sum

$$A_n(x) \equiv \sum_{k=0}^n a_k x^k. \quad (\text{A.2})$$

Being asymptotic means that at any given $x \neq 0$, one has $A_n(x) \rightarrow \infty$ as $n \rightarrow \infty$. In this case, one might resort to the Borel summation method by defining the Borel transform of $A(x)$ as [23]

$$\mathcal{B}A(t) \equiv \sum_{k=0}^{\infty} \frac{a_k}{k!} t^k. \quad (\text{A.3})$$

If $\mathcal{B}A(t)$ converges for any positive t , or, if it converges for sufficiently small t to an analytic function that can be analytically continued to all $t > 0$, and if the integral

$$\int_0^{\infty} dt \exp(-t) \mathcal{B}A(tx) \quad (\text{A.4})$$

exists and equals $A_B(x)$ (where the subscript B stands for Borel), then we say that the Borel sum of the series on the right hand side of Eq. (A.1) is $A_B(x)$. It is not difficult to see that if the original series converges, i.e., if $\lim_{n \rightarrow \infty} A_n(x) = A(x) < \infty$, then $A_B(x) = A(x)$. Applying the above formalism to Eq. (28), we get

$$\begin{aligned} b_{0B}(\theta, \omega) &= \int_0^{\infty} dt \exp(-t) \sum_{k=0}^{\infty} \frac{c_{0,k}(\theta, \omega)}{k!} (t\sqrt{m})^k \\ &= \frac{1}{\sqrt{m}} \int_0^{\infty} dy \exp(-y/\sqrt{m}) \sum_{k=0}^{\infty} \frac{c_{0,k}(\theta)}{k!} y^k. \end{aligned} \quad (\text{A.5})$$

The last integral is to be computed numerically. One has to truncate the series at a certain order $k = k_{\text{trunc}}$, and to extend the integral over y up to a given value y_M , which is chosen such that the integrand becomes negligible for $y > y_M$. However, contrary to what happens in the original series, we found that the sum in the last integral converges, at least for all y -values smaller than y_M that are necessary to compute the integral. We do not know the function to which our Borel transform converges, and the corresponding radius of convergence, but the numerical results show that our series is Borel summable. The left panel of Fig. A1 shows the result of computing the density

$$n(\theta) = \int_{-\infty}^{\infty} d\omega \mathcal{G}(\omega) b_{0B}(\theta, \omega) \quad (\text{A.6})$$

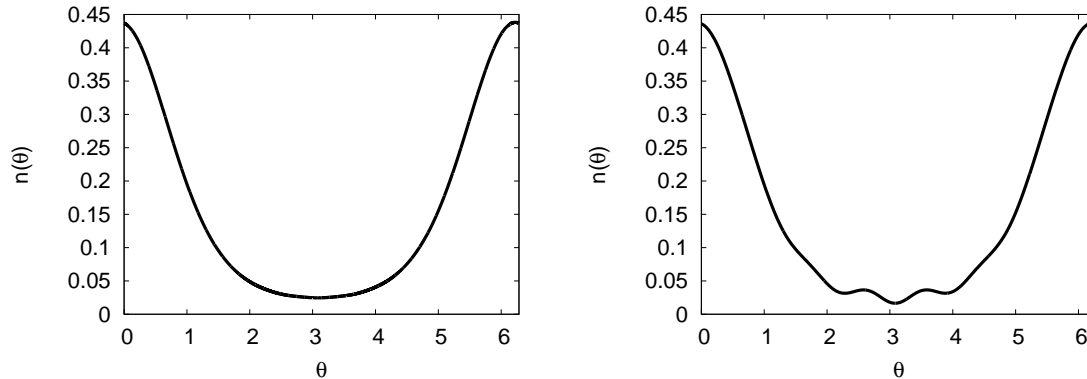


Figure A1. Density $n(\theta)$ in the dynamics (12), with $\tilde{u}_1 = 1$, $\tilde{u}_{s>1} = 0$, a Gaussian $\mathcal{G}(\omega)$, $m = 0.25$, $T = 0.25$, $\sigma = 0.295$. The left panel involves theoretical predictions using the Borel summation method with $k_{\text{trunc}} = 38$, while the right panel involves those using direct summation with $k_{\text{trunc}} = 22$.

m	0.0625	0.125	0.25	0.5	1.0
k_{max}	60	32	18	10	6

Table A1. For the dynamics, Eq. (12), with $\tilde{u}_1 = 1$, $\tilde{u}_{s>1} = 0$, and a Gaussian $\mathcal{G}(\omega)$, the table shows the maximum truncation order k_{max} in the computation of the density $n(\theta)$ as a function of m at a given representative $(\sigma, T) \equiv (0.295, 0.25)$ for which one observes a perfect agreement of the density $n(\theta)$ in theory and simulations, as in Fig. (2). The agreement gets worse and worse on successively increasing truncation order beyond k_{max} .

for the same conditions as in the left panel of Fig. 2, by truncating the sum in Eq. (A.5) at $k_{\text{trunc}} = 38$; the plot coincides with the one shown in the left panel of Fig. 2. On the other hand, summing the series (28) for $n = 0$ without resorting to the Borel summation method, and then computing the density $n(\theta)$, the result in the right panel of Fig. A1 shows that already for truncation order $k_{\text{trunc}} = 22$ of the series, one observes instabilities that get worse and worse with further increase of the truncation order (see Table A1 listing the truncation order k_{max} as a function of m , for the same representative $(\sigma, T) \equiv (0.295, 0.25)$ as in Fig. (2), up to which one observes a perfect agreement of the density $n(\theta)$ between theory and simulations). We conclude from this analysis that the series (28), although asymptotic, is effectively summable by the Borel summation method.

References

- [1] M. Bier, B. M. Bakker, and H. V. Westerhoff, *Biophys. J.* **78**, 1087 (2000).
- [2] A. T. Winfree, *The Geometry of Biological Time*, Springer, New York, 1980.
- [3] J. Buck, *Quart. Rev. Biol.* **63**, 265 (1988).
- [4] K. Wiesenfeld, P. Colet, and S. H. Strogatz, *Phys. Rev. E* **57**, 1563 (1998).

- [5] J. Javaloyes, M. Perrin, and A. Politi, *Phys. Rev. E* **78**, 011108 (2008).
- [6] S. Y. Ha, E. Jeong, and M. J. Kang, *Nonlinearity* **23**, 3139 (2010).
- [7] B. Eckhardt, E. Ott, S. H. Strogatz, D. M. Abrams, and A. McRobie, *Phys. Rev. E* **75**, 021110 (2007).
- [8] Z. Nédá, E. Ravasz, T. Vicsek, Y. Brechet, and A. L. Barabási, *Phys. Rev. E* **61**, 6987 (2000).
- [9] S. H. Strogatz, *Sync: The Emerging Science of Spontaneous Order* (Hyperion, New York, 2003).
- [10] Y. Kuramoto, in *International Symposium on Mathematical Problems in Theoretical Physics*, Lecture Notes in Physics, Vol. 39, ed. H. Arakai, Springer, New York, 1975.
- [11] Y. Kuramoto, *Chemical oscillations, Waves and Turbulence* (Springer, Berlin, 1984).
- [12] S. H. Strogatz, *Physica D* **143**, 1 (2000); J. A. Acebrón, L. L. Bonilla, C. J. Pérez Vicente, F. Ritort, and R. Spigler, *Rev. Mod. Phys.* **77**, 137 (2005).
- [13] B. Ermentrout, *J. Math. Biol.* **29**, 571 (1991).
- [14] J. A. Acebrón, L. L. Bonilla, and R. Spigler, *Phys. Rev. E* **62**, 3437 (2000).
- [15] J. A. Acebrón, and R. Spigler, *Phys. Rev. Lett.* **81**, 2229 (1998).
- [16] G. Filatrella, A. H. Nielsen, and N. F. Pedersen, *Eur Phys J B* **61**, 485 (2008).
- [17] M. Rohden, A. Sorge, M. Timme, and D. Witthaut, *Phys. Rev. Lett.* **109**, 064101 (2012).
- [18] S. Gupta, A. Campa, and S. Ruffo, *Phys. Rev. E* **89**, 022123 (2014).
- [19] S. Gupta, A. Campa, and S. Ruffo, *J. Stat. Mech.* **R08001** (2014).
- [20] B. Derrida, M. R. Evans, V. Hakim, and V. Pasquier, *J. Phys. A: Math. Gen.*, **26**, 1493 (1993).
- [21] V. Privman, *Nonequilibrium Statistical Mechanics in One Dimension* (Cambridge University Press, Cambridge, 2005).
- [22] H. Risken, *The Fokker-Planck Equation: Methods of Solution and Applications* (Springer, Berlin, 1996).
- [23] G. H. Hardy, *Divergent Series* (Chelsea Publishing Co., New York, 1991).
- [24] Mean-field interactions are a special case of long-range interactions. Interactions are called long-range when they decay asymptotically with the interparticle distance r as $r^{-\alpha}$ with $0 \leq \alpha \leq d$ in d dimensions, see, e.g., A. Campa, T. Dauxois, D. Fanelli, and S. Ruffo, *Physics of Long-Range Interacting Systems* (Oxford University Press, UK, 2014). The case $\alpha = 0$ corresponds to a mean-field interaction.
- [25] This ensures that the force on the i th rotator due to the j th one is equal and opposite to that on the j th rotator due to the i th, as required by the Newton's third law.
- [26] H. Sakaguchi, *Prog. Theor. Phys.* **79**, 39 (1988).
- [27] We will from now on take unity for the Boltzmann constant k_B .
- [28] H. C. Brinkman, *Physica* **22**, 29 (1956).
- [29] X. Durang, C. Kwon, and H. Park, arXiv:1309.5750.
- [30] K. Huang, *Statistical Mechanics* (Wiley, New York, 1987).
- [31] L. Golub and J. M. Pasachoff, *The Solar Corona, 2nd ed.* (Cambridge University Press, Cambridge, 2009).
- [32] P. C. Myers and G. A. Fuller, *The Astrophysical Journal* **396**, 631 (1992); A. A. Goodman *et al.*, *The Astrophysical Journal* **504**, 223 (1998); J. E. Pineda *et al.*, *The Astrophysical Journal Letters* **712**, L116 (2010).
- [33] L. Casetti and S. Gupta, *Eur. Phys. J. B* **87**, 91 (2014).
- [34] T. N. Teles, S. Gupta, and L. Casetti, arXiv:1502.04051.
- [35] O. E. Omel'chenko and M. Wolfrum, *Phys. Rev. Lett.* **109**, 164101 (2012).
- [36] M. Komarov, S. Gupta, and A. Pikovsky, *Europhys. Lett.* **106**, 40003 (2014).